Isotropic−Nematic Phase Separation in Suspensions of Polydisperse Colloidal Platelets

F. M. van der Kooij, D. van der Beek, and H. N. W. Lekkerkerker*

Van't Hoff Laboratory for Physical and Colloid Chemistry, Debye Institute, Utrecht University, Padualaan 8, 3584 CH Utrecht, The Netherlands

Received: August 31, 2000; In Final Form: November 30, 2000

We are studying the phase behavior of a suspension of platelike colloids which has a very broad size distribution, particularly in thickness. This suspension exhibits an isotropic−nematic phase separation over a notably wide range of particle concentrations, displaying a remarkable phenomenon. In part of the coexistence region, phase separation yields a nematic *upper* phase in coexistence with an isotropic *bottom* phase. If the nematic phase is isolated and diluted, the reverse situation is observed such that the isotropic phase now becomes the upper phase. We show that these phenomena can be explained by a pronounced fractionation with respect to platelet thickness.

1. Introduction

Suspensions of rod- or platelike colloidal particles may exhibit a spontaneous transition from a disordered isotropic (*I*) phase to an orientationally ordered nematic (*N*) phase. As noted by Onsager in the 1940s, this transition can be explained on purely entropic grounds.[1] The stability of the nematic phase stems from the fact that, at higher particle concentrations, the loss of orientational entropy associated with particle alignment is outweighed by the simultaneous gain in excluded volume (configurational) entropy. Although Onsager's theoretical approach was inspired by experimental observations of *I*−*N* phase separation in suspensions of rodlike particles,[2] as well as suspensions of platelike colloids,[3] the presently known examples of *I*−*N* phase separating suspensions almost exclusively deal with particles of rodlike shape.[2,4−11] In fact, Langmuir's observation of an *I*−*N* transition in suspensions of clay platelets (1938),[3] to which Onsager refers, later led to a contentious discussion as to why such suspensions more generally seem to form gels rather than to exhibit isotropic−nematic phase separation.[12,13] Recently, an alternative model system for platelike colloids has been developed, consisting of sterically stabilized gibbsite ($Al(OH)_3$) platelets.[14] These suspensions show an *I*−*N* transition which is not impeded by gelation, at densities which are in fair agreement with computer simulations for hard plates, i.e. plates that interact through a simple short-ranged repulsion.

The paucity of experimental platelet systems which exhibit the *I*−*N* transition,[3,14] and the (probably related) small number of simulation studies that have been conducted in this area,[15,16] leaves some elemental questions unanswered. For instance, little is known about the effect of polydispersity on the *I*−*N* transition. If we define the polydispersity, σ, as the standard deviation of the size distribution divided by the mean, the main effect of polydispersity on the *I*−*N* transition, that has come to light from experiments on the aforementioned gibbsite platelets ($\sigma \simeq 0.25$)[14] and from computer simulations ($0 < \sigma < 0.25$),[16] is a broadening of the *I*−*N* coexistence region. The computer simulation data showed that the width of the coexistence region depends quadratically on the polydispersity in diameter.[16] Yet, size segregation between the coexisting phases is weak in both experiment and simulation.

In this study, we aim to investigate the phase behavior of platelet suspensions with high polydispersity. A suspension of gibbsite platelets was synthesized using a slightly adapted preparation method; this yielded a wide, highly asymmetric size distribution, particularly in the platelets' thickness. We examine the effect of such a pronounced polydispersity on the width of the coexistence region, the occurrence of size fractionation, and, in analogy with observations for suspensions of polydisperse rods,[17−21] the possibility of an additional nematic phase that is induced by polydispersity.

2. Experimental Section

A suspension of sterically stabilized gibbsite ($Al(OH)_3$) platelets was prepared following the method described,[14,22] except for a slight change in the autoclaving procedure. In the first step of the synthesis, an aqueous suspension of gibbsite is prepared by the hydrothermal treatment of a 0.09 M HCl solution, which contains 0.08 M aluminum *sec*-butoxide and 0.08 M aluminum isopropoxide, for 72 h at 85 °C.[14,23−25] In the previously adopted method a Parr 4521 autoclave was used, comprised of a single Teflon vessel with stainless steel tubing hanging in the solution during the hydrothermal treatment. The presently employed autoclave consists of a set of Teflon vessels, enclosed in steel containers, which are heated in an oven while being subjected to a continuous slow rotation. After autoclaving and dialysis, the platelets were grafted by the usual method using a polyamine-modified polyisobutylene ($M_n \approx 1000$ g/mol) which was provided by Shell Research Ltd.[14,22] The thickness of the polymer layer has been estimated at 4 nm.[26]

A transmission electron microscope (TEM) micrograph of the platelets is reproduced in Figure 1a. It displays a significant number of very thick platelets, which are often found in a sidewise orientation on the TEM grid (as opposed to the flat orientation of thinner platelets). These thick platelets are virtually absent on TEM images of suspensions that were synthesized by the previously employed autoclave.[14,22,27−29] A quantitative determination of the platelets' thickness distribution is not straightforward however, as the thinner platelets are hardly ever viewed edgewise on TEM images. To promote the edgewise

* Author to whom correspondence should be addressed.

10.1021/jp0031597 CCC: $20.00
Published on Web 02/08/2001

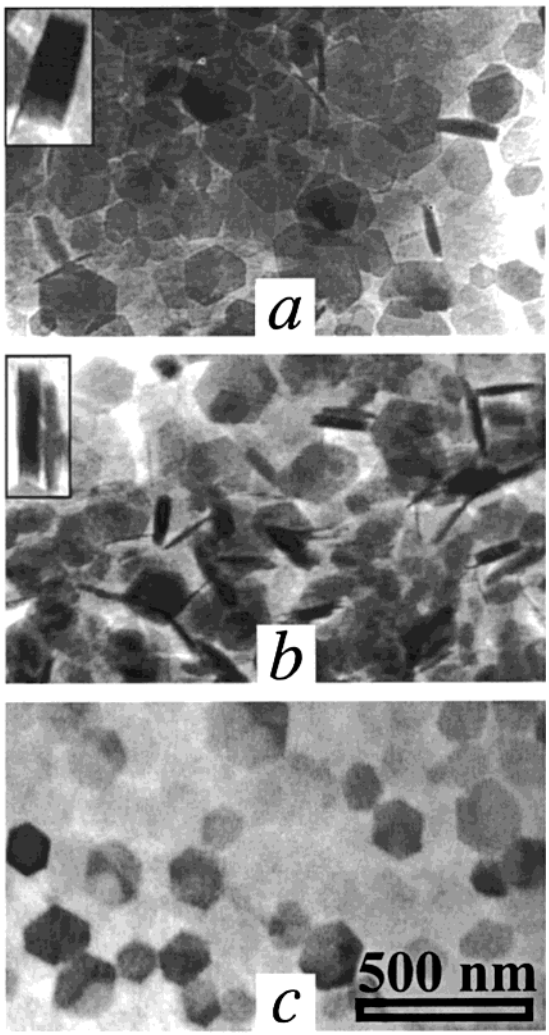

Figure 1. TEM images of the studied suspensions. (a) the overall system, (b) the latter's isotropic phase (Frac*I*), and (c) the coexisting nematic phase (Frac*N*). The scale bar (lower) applies to each of the images a−c. The inset in a and b depicts sidewise imaged platelets, at double magnification.

orientation of the whole particle population on the TEM grid, we deliberately flocculated samples by adding water prior to the determination of the thickness by TEM. The resulting distribution of L, which we define by the thickness of the core plus twice the polymer layer thickness, is shown in Figure 2. The number-average $\langle L\rangle$ and its relative standard deviation $\sigma_L = (\langle L^2\rangle - \langle L\rangle^2)^{1/2}/\langle L\rangle$ are given in Table 1.

Unlike the thickness, the diameter distribution resembles that of previously prepared suspensions. The diameter of the hexagonal gibbsite platelets is determined from TEM micrographs of unflocculated samples, as the mean of the three distances between opposite corners. The number-average particle diameter $\langle D\rangle$, which includes twice the width of the polymer layer, and the relative standard deviation σ_D are presented in Table 1. The diameter distribution is shown in Figure 2.

The particle volume fraction ϕ, which includes the solvent present in the grafted polymer layer, is calculated from the mass concentration c (determined by drying a known amount of dispersion at 75 °C to constant weight) according to[9,28]

$$\phi = \phi_{\text{core}}\frac{V_{\text{p}}}{V_{\text{core}}} = \frac{c(1-x)}{\rho_{\text{core}}}\frac{D^2L}{D_{\text{core}}^2L_{\text{core}}} = \frac{c}{\rho_{\text{p}}^{\text{eff}}} \qquad (1)$$

where V_{p} and V_{core} refer to the volume of the grafted particle and the gibbsite core, respectively. Further, x is the polymer mass fraction of grafted particles as obtained from elemental analysis (Table 2), ρ_{core} is the mass density of gibbsite (2.42 g/cm^3),[30] and D_{core} and L_{core} are the diameter and thickness of the core, respectively. This yields a mass density of the grafted particles $\rho_{\text{p}}^{\text{eff}} = 1.7$ g/cm^3 with an estimated error of 10% due to the uncertainty in polymer layer thickness.

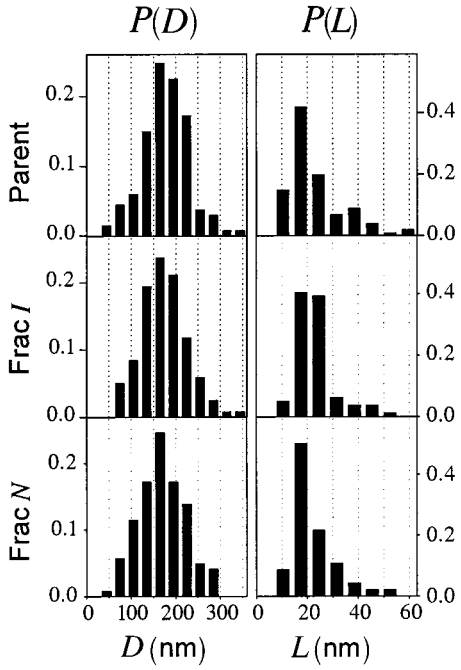

Figure 2. The diameter and thickness distribution of the grafted particles, as determined for the parent suspension, the isotropic phase (Frac*I*), and the nematic phase (Frac*N*). Note that the thickness distributions are determined from edgewise imaged platelets on TEM micrographs, which may give nonrepresentative results.

TABLE 1: The Mean Diameter and Standard Deviation of the Grafted Platelets in the Parent Suspension, and Its Coexisting Isotropic and Nematic Phases[a]

	$\langle D\rangle$ (nm)	σ_D (%)	$\langle L\rangle$ (nm)	σ_L (%)
parent	178	33	24	50
Frac*I*	174	30	24	42
Frac*N*	171	30	21	43

[a] The determination of the diameter is based on about 120 particles in each case. The thickness is based on 50−100 particles. The differences in $\langle L\rangle$ between the systems are therefore not significant, and values for σ_L have only qualitative meaning.

TABLE 2: Results from Elemental Analysis and Density Measurements[a]

	elemental analysis					
	Al	C	H	N	x	ρ_{p} (g/cm^3)
parent	0.2918	0.1180	0.0098	0.0540	0.1456	
ungrafted	0.3269	0.0014	0.0000	0.0392		
Frac*I*	0.2891	0.1154	0.0095	0.0527	0.1417	2.050
Frac*N*	0.2887	0.1220	0.0099	0.0535	0.1495	2.027

[a] Depicted are the mass fractions of some elements and the mass fraction of polymer x. The latter is calculated by adding the C, H, and N contents of the grafted particles after correction for the C, H, and N contents in the bare particles before grafting.

3. Isotropic−Nematic Phase Separation Results

3.1. Parent Suspension. Up to volume fraction $\phi = 0.18$ the platelet suspension is in the isotropic state, whereas above $\phi = 0.31$ it is fully nematic. $I-N$ coexistence, which is observed

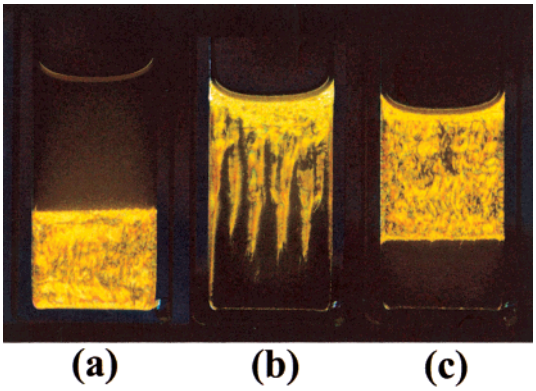

Figure 3. Samples after $I-N$ phase separation as observed between crossed polarizers. Volume fractions of the samples vary from (a) $\phi = 0.22$, (b) $\phi = 0.24$, to (c) $\phi = 0.25$.

for intermediate volume fractions, presents a surprising feature. Between $\phi = 0.18$ and $\phi = 0.24$, phase separation yields an isotropic upper phase and a nematic bottom phase (Figure 3a); this is similar to other cases of $I-N$ phase separation cited in the literature.[2,4−11,14] However from $\phi = 0.24$ up to the completely nematic state, the nematic phase becomes the *upper* phase which coexists with an isotropic *bottom* phase (Figure 3c). This implies that the nematic phase has a lower mass density than the coexisting isotropic phase. The origin of this anomalous behavior is discussed in the next section.

Consequently, for $\phi = 0.24$, we observe coexistence of an isotropic and a nematic phase of almost equal mass density. One indication of the mass density difference being very small is that the $I-N$ interface is no longer sharp (Figure 3b). The large surface of the indented interface also points to a very low interfacial tension. Indeed, the interfacial tension, which is estimated by[31,32] $\gamma \simeq k_B T\phi/\xi^2$, with $k_B T$ equal to the thermal energy and ξ equal to the typical interfacial thickness, is generally extremely small in colloidal suspensions because ξ (typically of the order of the size of the colloidal particles) is much larger than in molecular systems. In the present case this gives an interfacial tension roughly in the range $0.01-0.1$ μN/m, such that its effect on the shape of the interface is indeed very small. The actual shape of the $I-N$ interface, that it is indented (Figure 3b), is an indication that the heavier particles in the nematic phase have started sedimenting to the bottom of the phase. This toothlike interface appears a few days after the initial macroscopic separation of a nematic upper phase and an isotropic upper phase, which are divided by an indeterminate interface. Furthermore, the minor mass density difference between the coexisting phases causes the time scale for macroscopic phase separation to increase from a maximum of 2 d, both below and above $\phi = 0.24$, to several days at $\phi = 0.24$.

A striking feature of the $I-N$ transition is the width of the biphasic gap (Figure 4). If we define the width as $\Delta\phi/\phi$, i.e. the volume fraction difference between the I and N phase boundary divided by their mean, we find $\Delta\phi/\phi \approx 0.5$. For comparison, we note that earlier observations for gibbsite platelets with of 25 and 17% polydispersity in diameter yielded $\Delta\phi/\phi \approx 0.16$ and 0.05, respectively.[33]

The suspension's phase behavior, which is studied up to the viscosity-limited volume fraction $\phi = 0.45$, comprises only an isotropic and a nematic phase. Hence we find no indications for a columnar phase, which was found earlier for gibbsite platelet suspensions of lower polydispersity (up to $\sigma_D = 0.25$).[33]

3.2. Fractionated Suspensions. To investigate the nature of the upper nematic and the lower isotropic phases, the suspension

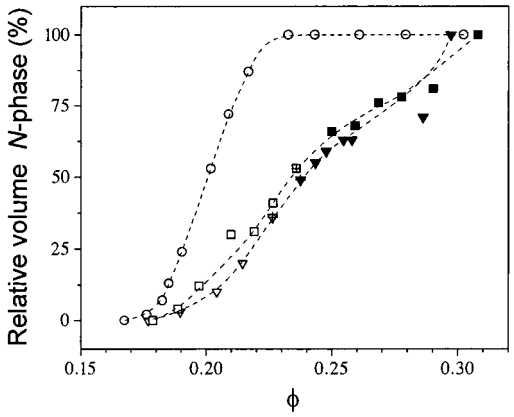

Figure 4. Relative volume of the nematic phase as a function of the platelet volume fraction. Symbols correspond to the parent suspension (□), the subsystem Frac$I$ (▽), and subsystem Frac$N$ (○). Open symbols indicate that the isotropic phase is on top of the nematic phase, whereas closed symbols indicate the opposite. The + sign marks the situation in which the coexisting phases are approximately equal in mass density, leading to phase separation of the kind depicted in Figure 3b.

is brought to $\phi = 0.29$ and is left to phase separate. The nematic upper phase is subsequently separated from the isotropic bottom phase, which enables us to determine the properties of the individual phases. We denote the isolated isotropic and nematic phases by Frac$I$ and Frac$N$, respectively. Consistent with the isotropic and nematic being the lower and upper phase, respectively, their mass densities are $\rho_I = 1.156 \pm 0.002$ $\rho_N = 1.146 \pm 0.002$ g/cm^3. TEM images of the separated isotropic and nematic phases are shown in Figure 1. The main conclusion from the TEM is that the exceptionally thick platelets of the parent suspension are, to a large extent, expelled from the nematic phase while they preferentially occupy the isotropic phase. Diameter and thickness distributions that were determined from the TEM images are shown in Figure 2. The diameter of the platelets is practically indistinguishable in the parent system and in both the Frac$I$ and Frac$N$ subsystems. On the other hand, the thickness of the platelets is undeniably fractionated, as the Frac$I$ subsystem is notably enriched by platelets in the thickness range of 22−27 nm. The quantitative validity of the measured thickness distribution may be limited however. This is because the method used to determine the thickness, which is done by measuring the width of the platelets that are found in a sidewise orientation on the TEM grid, is probably not representative. It may, to some extent, exclude the thinner platelets which have a lower chance of being found in an edgewise orientation. Inspection of the TEM images suggests that fractionation with respect to platelet thickness is indeed much more pronounced than what is presented by the measured distributions. A more objective (albeit qualitative) examination of the fractionation is provided by the phase behavior of the Frac$I$ and Frac$N$ subsystems. As depicted in Figure 4, the $I-N$ transition exhibited by the Frac$I$ system shows a remarkable resemblance to the parent suspension. The Frac$N$ suspension, on the other hand, has a much narrower $I-N$ coexistence region ($\Delta\phi/\phi \approx 0.25$), which demonstrates that its polydispersity in diameter or thickness (or both) is largely reduced. However, as noted earlier, the diameter distributions in the parent, Frac$I$ and Frac$N$ systems are virtually identical (Figure 2). This implies that it is particularly the thickness of the platelets that is fractionated at the transition. In fact, the biphasic gap starts at around the same volume fraction as in the parent system, while the completely nematic state is reached at much lower volume fraction. Intuitively, the latter shows us that the number of thick (low

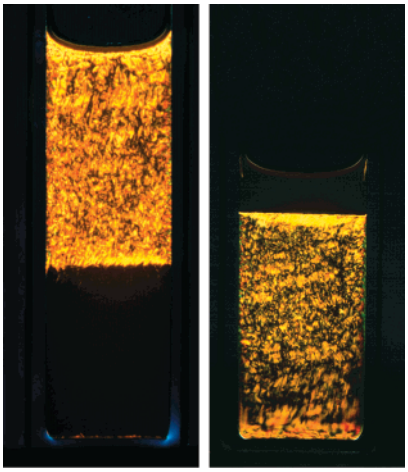

Figure 5. The $I-N$ transition in (a) is the Frac$I$ and (b) is the Frac$N$ system, at $\phi = 0.24$ and $\phi = 0.22$ respectively. Pictures taken between crossed polarizers.

D/L) platelets is strongly reduced in the Frac$N$ subsystem, as compared to the parent suspension.

Finally, a striking feature of the Frac$N$ suspension is that it does not exhibit phase separation between a nematic *upper* phase and an isotropic *lower* phase at any point in the $I-N$ coexistence region (Figure 5). This is an implicit result of the Frac$N$ system's lower polydispersity and its subsequently weaker extent of fractionation, which, in the following, is interpreted as the origin of the anomalous $I-N$ transition in the parent and the Frac$I$ suspensions.

4. Discussion

Computer simulations of monodisperse, infinitely thin platelets have shown that the coexisting densities and pressure at the $I-N$ transition are[16]

$$n_I D^3 \simeq 3.7, \qquad n_N D^3 \simeq 4.0, \qquad \tilde{\Pi} \simeq 15 \tag{2}$$

where n_I and n_N are the number densities of platelets in the isotropic and the nematic phase, respectively, and $\tilde{\Pi} = \Pi D^3/kT$ is the reduced osmotic pressure. On the other hand, in the case of platelets with a finite thickness ($D/L = 10$) these quantities are

$$n_I D^3 \simeq 3.8, \qquad n_N D^3 \simeq 3.9, \qquad \tilde{\Pi} \simeq 32 \tag{3}$$

The reduced coexisting densities at the transition are thus virtually independent of the thickness L, while the reduced osmotic pressure at the transition increases strongly with the plate thickness. Let us consider how this difference in pressure affects the $I-N$ transition in systems which comprise both thick and thin platelets, in particular, with respect to fractionation. For such systems no relevant theory, simulations, or experiments have been reported so far. However, theory exists for the case of binary mixtures of thick and thin rods with equal length. Thick rods exhibit the $I-N$ transition at a lower pressure than thin rods.[20,34] From the shape of the pressure−composition diagram of a binary rod mixture (see ref 20 for details), it follows that fractionation occurs, with the thick rods accumulating in the nematic phase. If we now consider a binary mixture of thick and thin platelets, where the thick particles exhibit the $I-N$ transition at the *higher* pressure, we may use the (mirrored) form of the binary rod pressure−composition diagram to estimate the $I-N$ transition for the case of the platelets (sketched in Figure 6). Like rods, platelets will exhibit fractionation with respect to thickness. In the case of platelets, however, the thicker particles will accumulate in the isotropic phase. This agrees with the experimental observations for the presently studied platelet suspension.

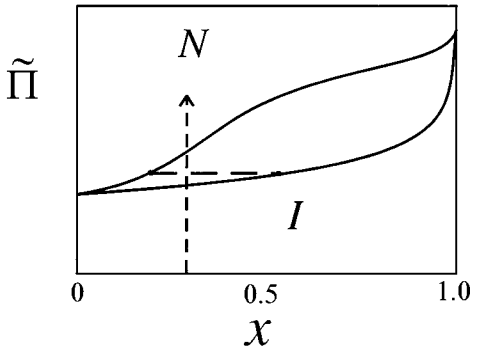

Figure 6. Schematic representation of the estimated phase diagram of a binary mixture of thick and thin platelets, presented as the reduced pressure ($\tilde{\Pi} = \Pi D^3/kT$) at the $I-N$ transition versus the composition $x = N_{\text{thick}}/(N_{\text{thick}} + N_{\text{thin}})$, with N_{thick} and N_{thin} equal to the numbers of thick and thin platelets, respectively. The dashed line for a certain composition, x, shows the effect of fractionation with respect to L. The coexisting points at the isotropic and the nematic branch (at common $\tilde{\Pi}$, as they are in thermodynamical equilibrium) are enriched and impoverished in the relative amount of thick platelets, respectively, corresponding to a larger/lower value of x.

But how does fractionation with respect to thickness relate to the experimentally observed anomalous behavior at the $I-N$ transition? As the particle mass density is virtually the same in the I and N phases (see Table 2), the observed nematic upper phase demonstrates that $\phi_I > \phi_N$ in such samples. Yet, at the same time, we can have $n_I D^3 < n_N D^3$ (for instance, see eq 7) since for disk-shaped particles ϕ and nD^3 are linked by

$$\phi = n\frac{\pi}{4}D^2L = \frac{\pi}{4}\frac{L}{D}nD^3 \tag{4}$$

which demonstrates that the remarkable phenomenon of a nematic upper phase can be understood if the aspect ratio of the platelets in the nematic phase is sufficiently higher than that in the coexisting isotropic phase. More precisely, in the case of polydisperse particles eq 4 becomes

$$\phi = n\frac{\pi}{4}\frac{\langle D^2L\rangle}{\langle D^3\rangle}\langle D^3\rangle \simeq \frac{\pi}{4}(1+2\sigma_D^2)^{-1}\frac{\langle L\rangle}{\langle D\rangle}n\langle D^3\rangle \tag{5}$$

where $\langle D^3\rangle/\langle D\rangle^3 = 1 + 3\sigma_D^2$ and $\langle D^2\rangle/\langle D\rangle^2 = 1 + \sigma_D^2$ are used for symmetric distributions, and where D and L are assumed to be uncorrelated. Since σ_D is almost equal in the I and N phases, the observation that $\phi_I > \phi_N$ implies that

$$\frac{\phi_I}{\phi_N} \simeq \frac{(n\langle D^3\rangle)_I}{(n\langle D^3\rangle)_N}\frac{\langle L\rangle/\langle D\rangle_{\text{I}}}{\langle L\rangle/\langle D\rangle_{\text{N}}} > 1 \tag{6}$$

As fractionation with respect to D is practically absent in the experiment, fractionation with respect to L must be strong enough to overrule the thermodynamical density difference $(n\langle D^3\rangle)_I < (n\langle D^3\rangle)_N$. For the experimental system, this density difference will be larger than is suggested by eq 2, as a result of polydispersity, and will also depend on the current place in the coexistence region. In the case of 25% polydispersity in diameter, the coexisting densities, found by computer simulations, for infinitely thin hexagonal platelets are[35]

$$(n\langle D^3\rangle)_I \simeq 3.0, \qquad (n\langle D^3\rangle)_N \simeq 4.4 \tag{7}$$

However, for a system of hexagonal platelets with polydispersity in both diameter and thickness, these values are unknown, and hence the extent of fractionation that is required to meet the condition of eq 6 is not quantitatively known .

Furthermore, a marked feature of the observed $I-N$ transition is that the nematic phase becomes the upper phase only in the higher concentration part of the $I-N$ coexistence region. This observation can also be understood within the framework of our argumentation. From the TEM micrographs (and to some extent, the measured thickness distribution determined therefrom) we know that the thickness distribution is asymmetric, in the sense that the relative amount of very thick platelets is small. This situation corresponds to a point close to $x = 0$ in the $\tilde{\Pi} - x$ diagram (Figure 6). Upon increasing ϕ (hence, going up in $\tilde{\Pi}$ at fixed x) we see that after entering the $I-N$ coexistence region the difference in x of the coexisting phases increases until the fully nematic state is reached. Hence, there may be a threshold ϕ above which fractionation becomes strong enough to fulfill eq 6, as indicated by the experiment. Likewise, the Frac*N* suspension (which is represented by a lower value of x than that of the parent system) is not found to exhibit a nematic upper phase anywhere in its $I-N$ coexistence region, since the difference in x of its coexisting phases is apparently never large enough.

The overall topology of the suspension's phase diagram is relatively simple, as it comprises only an isotropic region, a region of $I-N$ coexistence, and a nematic region. Apparently, no demixing of the nematic phase into two separate nematic phases of differing density and composition occurs, despite the platelets' considerable polydispersity in thickness and diameter. We may compare this observation to the effect of polydispersity on the phase behavior of rods, which has received ample attention in both theory and simulations. There, $N-N$ demixing has been found for the case of mixtures of short and long rods,[17,36] for thick and thin rods,[18−20,34] and for rods which differ in both length and diameter.[21] Experimentally, $N-N$ demixing has indeed been observed for length-polydisperse rods, in suspensions of schizophyllan[37] and imogolite,[38] but not for diameter-polydisperse rods. Thus, the absence of $N-N$ demixing in the present case of (particularly thickness-)polydisperse platelets raises an interesting question for further theoretical study and simulations; that is, to address the extent of thickness and diameter polydispersity required for such demixing to occur in the case of platelets. Another striking feature of the phase diagram, which is studied up to $\phi = 0.45$, is the lack of a columnar phase. Recently a columnar phase has been observed for less polydisperse ($\sigma_D \leq 0.25$) gibbsite platelets;[33] the role of diameter (and thickness) polydispersity in the suppression of the columnar phase is hence another issue to be addressed in theory and simulations.

5. Conclusions

We have studied the phase behavior of a suspension of platelets with a size distribution which is both very broad and highly asymmetric, particularly in the platelet thickness. Due to this polydispersity, the width of the $I-N$ coexistence region is several times broader than what has been found earlier for suspensions of lower polydispersity. A surprising feature of the $I-N$ transition is that it, at least in part of the coexistence region, yields a nematic upper phase and an isotropic bottom phase. Furthermore, if the nematic phase is isolated from the coexisting isotropic phase, this system displays a much narrower $I-N$ gap width and the isotropic phase is now the upper phase throughout the coexistence region. We show that these phenomena can, in principle, be explained on the basis of strong fractionation with respect to the platelets' thickness.

Despite the distinct effects on the $I-N$ transition, the platelets' polydispersity does not give rise to the appearance of $N-N$ demixing; this is a possibility which was previously noted for rods.[17−21,34,36] At the same time, the extent of polydispersity is apparently large enough to suppress the formation of a columnar phase in these suspensions. It would also be interesting to study these issues in theory and simulations, to gain more insight into the role of diameter and thickness polydispersity in $N-N$ demixing and the stability of a columnar phase.

Acknowledgment. We like to thank Gert-Jan Vroege for a critical reading of the manuscript. This work was supported by the foundation for Fundamental Research on Matter (FOM).

References and Notes

(1) Onsager, L. *Ann. N. Y. Acad. Sci*. **1949**, *51*, 627.
(2) Bernal, J. D.; Fankuchen, I. *J. Gen. Physiol*. **1941**, *25*, 111.
(3) Langmuir, I. *J. Chem. Phys*. **1938**, *6*, 873.
(4) Zocher, H. *Z. Anorg. Allg. Chem*. **1925**, *147*, 91.
(5) Pelletier, O.; Davidson, P.; Bourgaux, C.; Livage, J. *Europhys. Lett*. **1999**, *48*, 53.
(6) Kreibig, U.; Wetter, C. *Z. Naturforsch*. **1980**, *35*, 750.
(7) Fraden, S.; Hurd, A. J.; Meyer, R. B.; Cahoon, M.; Caspar, D. L. D. *J. Phys.* **1985**, 46.
(8) Maeda, Y.; Hachisu, S. *Colloids Surf.* **1983**, *7*, 357.
(9) van Bruggen, M. P. B.; Dhont, J. K. G.; Lekkerkerker, H. N. W. *Macromolecules* **1999**, *32*, 2256.
(10) Dong, X. M.; Kimura, T.; Revol, J. F.; Gray, D. G. *Langmuir* **1996**, *12*, 2076.
(11) Folda, T.; Hoffmann, H.; Chanzy, H.; Smith, P. *Nature* **1988**, *333*, 55.
(12) Gabriel, J. C. P.; Sanchez, C.; Davidson, P. *J. Phys. Chem*. **1996**, *100*, 11139.
(13) Mourchid, A.; Delville, A.; Lambard, J.; Lecolier, E.; Levitz, P. *Langmuir* **1995**, *11*, 1942.
(14) van der Kooij, F. M.; Lekkerkerker, H. N. W. *J. Phys. Chem. B* **1998**, *102*, 7829.
(15) Veerman, J. A. C.; Frenkel, D. *Phys. Rev. A* **1992**, *45*, 5632.
(16) Bates, M. A.; Frenkel, D. *J. Chem. Phys*. **1999**, *110*, 6553.
(17) Vroege, G. J.; Lekkerkerker, H. N. W. *J. Phys. Chem*. **1993**, *97*, 3601.
(18) van Roij, R.; Mulder, B. *Phys. Rev. E* **1996**, *54*, 6430.
(19) Dijkstra, M.; van Roij, R. *Phys. Rev. E* **1997**, *56*, 5594.
(20) van Roij, R.; Mulder, B.; Dijkstra, M. *Physica A* **1998**, *261*, 374.
(21) Hemmer, P. C. *Mol. Phys*. **1999**, *96*, 1153.
(22) van der Kooij, F. M.; Philipse, A. P.; Dhont, J. K. G. *Langmuir* **2000**, *16*, 5317−5323.
(23) Buining, P. A.; Pathmamanoharan, C.; Jansen, J. B. H.; Lekkerkerker, H. N. W. *J. Am. Ceram. Soc*. **1991**, *74*, 1303.
(24) Philipse, A. P.; Nechifor, A. M.; Patmamanoharan, C. *Langmuir* **1994**, *10*, 4451.
(25) Wierenga, A.; Lenstra, T. A. J.; Philipse, A. P. *Colloids Surf. A* **1998**, *134*, 359.
(26) Smits, C.; Briels, W. J.; Dhont, J. K. G.; Lekkerkerker, H. N. W. *Prog. Colloid. Polym. Sci.* **1989**, *79*, 287.
(27) van der Kooij, F. M.; Vogel, M.; Lekkerkerker, H. N. W. *Phys. Rev. E* **2000**, *62*, 5397.
(28) van der Kooij, F. M.; Boek, E. S.; Philipse, A. P., submitted to *J. Colloid Interface Sci*. **2000**.
(29) van der Kooij, F. M.; Lekkerkerker, H. N. W. *Phys. Rev. Lett*. **2000**, *84*, 781.
(30) Gitzen, W. H. *Alumina as a Ceramic Material*; The American Ceramic Society: Columbus, OH, 1970.
(31) van der Schoot, P. *J. Phys. Chem. B* **1999**, *103*, 8804.
(32) de Hoog, E. H. A.; Lekkerkerker, H. N. W.; Schulz, J.; Findenegg, G. H. *J. Phys. Chem. B* **1999**, *103*, 10657.
(33) van der Kooij, F. M.; Kassapidou, K.; Lekkerkerker, H. N. W. *Nature* **2000**, *406*, 868.
(34) Sear, R.; Jackson, G. *J. Chem. Phys*. **1995**, *103*, 8684.
(35) Bates, M. A. *J. Chem. Phys*. **1999**, *111*, 1732.
(36) van Roij, R.; Mulder, B. *J. Chem. Phys.* **1996**, *105*, 11237.
(37) Itou, T.; Teramoto, A. *Macromolecules* **1984**, *17*, 1419.
(38) Kajiwara, K.; Donkai, N.; Hiragi, Y.; Inagaki, H. *Makromol. Chem*. **1986**, *187*, 2883.